

# НАУКИ О ЗЕМЛЕ

УДК 550.42+552.333.2(620)

DOI 10.21440/2307-2091-2018-3-7-18

## GEOCHEMISTRY, URANIUM, THORIUM AND RARE EARTH ELEMENTS OF TRACHYTE DYKES OF UMM SALATIT MOUNTAIN AREA, CENTRAL EASTERN DESERT, EGYPT

**Mohamed Mahmoud Ghoneim<sup>1,2</sup>**

moh.gho@mail.ru

Saint Petersburg State University

Saint Petersburg, Russia

**Gehad Mohamed Saleh<sup>2</sup>,**

drgehad\_m@yahoo.com

**Maher Dawoud Dawoud<sup>3</sup>,**

dawoud\_99@yahoo.com

**Mohamed Saleh Azab<sup>2</sup>,**

mohamedazab68@yahoo.com

**Mahmoud Ahmed Mohamed<sup>2</sup>,**

hoodageo@yahoo.com

**Hamdy Ahmed Awad<sup>4,5</sup>**

hamdiawaad@gmail.com

<sup>1</sup>Saint Petersburg University, Saint Petersburg, Russia

<sup>2</sup>Nuclear Materials Authority, Cairo, Egypt

<sup>3</sup>Minufiya University, Faculty of Science, Geology Department,

Minufiya, Egypt

<sup>4</sup>South Federal University

Rostov on Don, Russia

<sup>5</sup>Al-Azhar University

Assiut, Egypt

Umm Salatit Mountain area is a part of the Central Eastern Desert of Egypt. It is composed of ophiolitic mélange, older granitoids, biotite granites, muscovite granites and post granitic dykes and veins.

**Purpose of the work.** The present work deals with the detailed investigations of the geology, petrography, geochemistry and spectrometric prospecting of the studied trachyte dykes as a possible source of uranium mineralization.

**Research methods.** This work involves both field work (Construction of geological map with the structural features, scale 1 : 50,000, Spectrometric measurements of the different rock units using a portable gamma-ray spectrometer RS-230) and laboratory work (preparation of thin sections for petrographic studies by polarizing microscope), Atomic Emission Spectroscopy (AES), and Mass-Spectrometer with Inductively Coupled Plasma (ICP-MS).

**Results.** Petrographically, trachyte dykes consist mainly of K-feldspar with relatively minor amount of plagioclase, iron oxides, quartz and biotite. Secondary minerals are represented by sericite, muscovite, chlorite, carbonates and epidote. Accessory minerals are represented by opaque minerals. Trachytic textures are the main characteristic feature in trachyte. Geochemically, the investigated trachyte dykes were originated from an alkali magma rich in total alkalis, and the tectonic setting is continental basalt. Trachyte dykes have steep LREEs, nearly flat HREEs and a negative Eu anomaly. The negative Eu anomaly is either due to the partitioning of Eu into feldspar during fractionation, which is an important process in developing alkalinity, or the presence of residual feldspar in the source. Another alternative explanation for the negative Eu anomaly is based on the high oxygen fugacity in the melt due to volatile saturation. In general, all trachyte samples show moderate enrichment of most large ion lithophile elements (LILE) and high field strength elements (HFSE) and depletion of P, Ti and K. The depletion of Ti and p is ascribed to fractionation of titanomagnetite and apatite. The determination of equivalent uranium, thorium (ppm), potassium % and dose rate (m Sv/y) radiometrically by using portable RS-230 indicates that the dose rate in the trachyte dykes ranges from 0.5 to 1.5 with an average of 1.2 (m Sv/y). The radiometric data of the radioelements for them show a wide variation in eU and eTh contents. The eU content ranges from 2 to 14 ppm with an average of 6.6 ppm and the eTh content ranges from 4 to 37 ppm with an average of 18.03 ppm. Both U and Th correlate similarly with other major and trace elements, reflecting their geochemical coherence during the crystallization of the magma.

**Keywords:** geochemistry, uranium, trachyte dykes, Egypt, Umm Salatit.

### Introduction

Umm Salatit Mountain area is a part of the Central Eastern Desert of Egypt. It is bounded by longitudes 33°45' and 33°60' E and latitudes 25°10' and 25°20' N, covering an area of 450 km<sup>2</sup>. The area is accessible from Idfu–Marsa Alam road. It is traversed by the main desert road of Barramiya–Gabal El Rukham originating southward from the main road of Idfu–Marsa Alam. It is composed of ophiolitic mélange, older granitoids, biotite granites, muscovite granites and post granitic dykes and veins (Fig. 1).

A lot of researches has been done about ophiolitic rocks, ophiolitic mélange and granitoid rocks but no one study in details the volcanic trachyte dykes which cut across muscovite granites and extend through several meters.

### Methodology

1 – Field work is accomplished construction of geological map with the structural features, scale 1 : 50,000 based on mosaic and field observations. It is also comprised the collection of the rock specimens from the different rock units through cross profiles covering the study area. Moreover, Spectrometric measurements of the different rock units using a portable gamma-ray spectrometer RS-230. 2 – Fifteen samples of trachyte dykes were chosen for preparation of thin sections for petrographic studies. The microscopic studies and photomicrographs were carried out using a Nikon (Optiphot-Pol) polarizing microscope equipped with a full automatic photomicrographic attachment (Microflex AFX-II). 3 – Representative seven samples trachyte dykes are selected for analyses of trace elements, REEs concentrations. These were prepared for complete chemical analysis by fused tablets

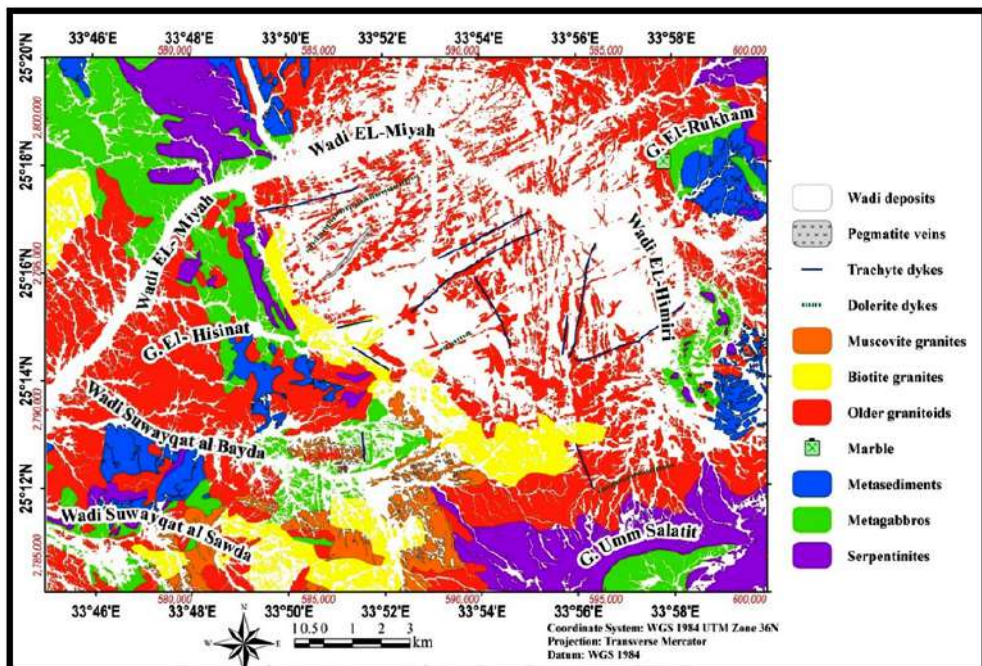


**Figure 1.** Geological map of Umm Salatit Mountain area, Central Eastern Desert, Egypt (after [1] modified after [2]).

Рисунок 1. Геологическая карта горного района Умм Салатит (Центральная часть Восточной пустыни), Египет (по [1], видоизмененный по [2]).

with  $\text{LiBO}_2$  and  $\text{HNO}_3$  dissolution in the laboratory of ACME Analytical Laboratories (Vancouver) Ltd, Canada using ICP-MS. The major elements were analyzed by using an Atomic Emission Spectroscopy (AES) coupled with Inductively Plasma (IP) source.

#### Geological setting and petrography of trachyte dykes

Trachyte dykes are the most abundant dyke rocks in the area. These dykes show variable trends to N-S and NNE-SSW trends. They are usually fine-grained, buff, pale brown to red, deep red and reddish brown in colour due to the degree of ferrugination. These dykes are altered, massive and range in thickness from 10 m to 20 m. They cut younger granitoids. Macroscopically, Trachyte dykes are fine to medium grained of buff and pale pink to red in colour. Microscopically, consist mainly of K-feldspar with relatively minor amount of plagioclase, iron oxides, quartz and biotite. Secondary minerals are represented by sericite, muscovite, chlorite, carbonates and epidote. Accessory minerals are represented by opaque minerals.

K-feldspar occurs as phenocrystals from orthoclase and perthite sometimes with twining in a matrix of anorthoclase and sanidine (Fig. 2, a, b and c). Sanidine feldspar, very commonly occurs in two generations, i. e. both as large well-shaped porphyritic crystals and smaller imperfect rods or laths forming a finely crystalline groundmass.

K-feldspars may occur as subparallel fluxional orientation forming trachytic texture or as randomly oriented crystals forming spherulitic texture (Fig. 2, d and e). Plagioclase is rare and form euhedral to subhedral crystals 0.5 × 3.5 mm in phenocryst and 0.3 × 0.8 in the groundmass. It ranges in composition from oligoclase to andesite ( $\text{An}_{13-38}$ ) shows glomeroporphyritic texture (Fig. 2, f) and altered to sassurite and calcite. They occur as patches distributed through the rocks. Quartz occurs as irregular anhedral crystals with corroded plagioclase and biotite and intergrowth with K-feldspar forming graphic texture. It may be also enclosed in biotite. Amygdales are present and filled by carbonates. According to [3], the term (granophytic) implies a graphic intergrowth of quartz and either K-feldspar or Na-rich feldspar, rather than a quartz and alkali-feldspar solid solution, although [4] regarded the term as the irregular, finer-grained counter part of the graphic intergrowth. It may be due to simultaneous crystallization of quartz and alkali feldspars. Biotite occurs as subhedral to euhedral flakes with one set of cleavage and strongly pleochroic from brown to dark brown in colour. It is subjected severe alteration to chlorite, muscovite, iron oxides and epidote. Carbonates occur as anhedral crystals or as fine grained. Opaque minerals occur as anhedral crystals in the fine-grained groundmass with K-feldspar, plagioclase and quartz.

#### Geochemistry of trachyte dykes. Geochemical Nomenclature

The geochemical nomenclature of the trachyte is studied by many workers elsewhere using the variation in the major oxides (wt. %) and trace elements (ppm).

The  $\text{Na}_2\text{O} + \text{K}_2\text{O}$  (wt. %) versus  $\text{SiO}_2$  (wt. %) diagram (Fig. 3) suggested by [5] shows that the analysed trachyte samples fall along the trachyte fields.

The contents of the major oxides, trace elements in the analyzed trachyte dykes as well as CIPW norms are given in (Table 1). The average chemical composition of the studied trachyte dykes when compared with world trachyte dykes [6] and trachyte of Umm Shaghir CED, Egypt [7] they show increasing in  $\text{SiO}_2$ ,  $\text{Fe}_2\text{O}_3$ ,  $\text{MgO}$ ,  $\text{Na}_2\text{O}$  and  $\text{CaO}$  but decreasing in  $\text{Al}_2\text{O}_3$ , when compared with Average of Um Domi trachytes [8] they show high  $\text{SiO}_2$ ,  $\text{Na}_2\text{O}$  and  $\text{Al}_2\text{O}_3$  contents and when compared with average of trachyte of G. El Ghorfa area, SED, Egypt [9] they show high  $\text{SiO}_2$  and  $\text{Al}_2\text{O}_3$  contents but low  $\text{Fe}_2\text{O}_3$  and  $\text{P}_2\text{O}_5$  contents (Table 2). The relative concentrations of trace elements in the studied rocks are shown in the form of a primitive mantle-normalized diagram (Fig. 4) based on the normalized factors of [10]. In general, all rocks show moderate enrichment of most large ion lithophile elements

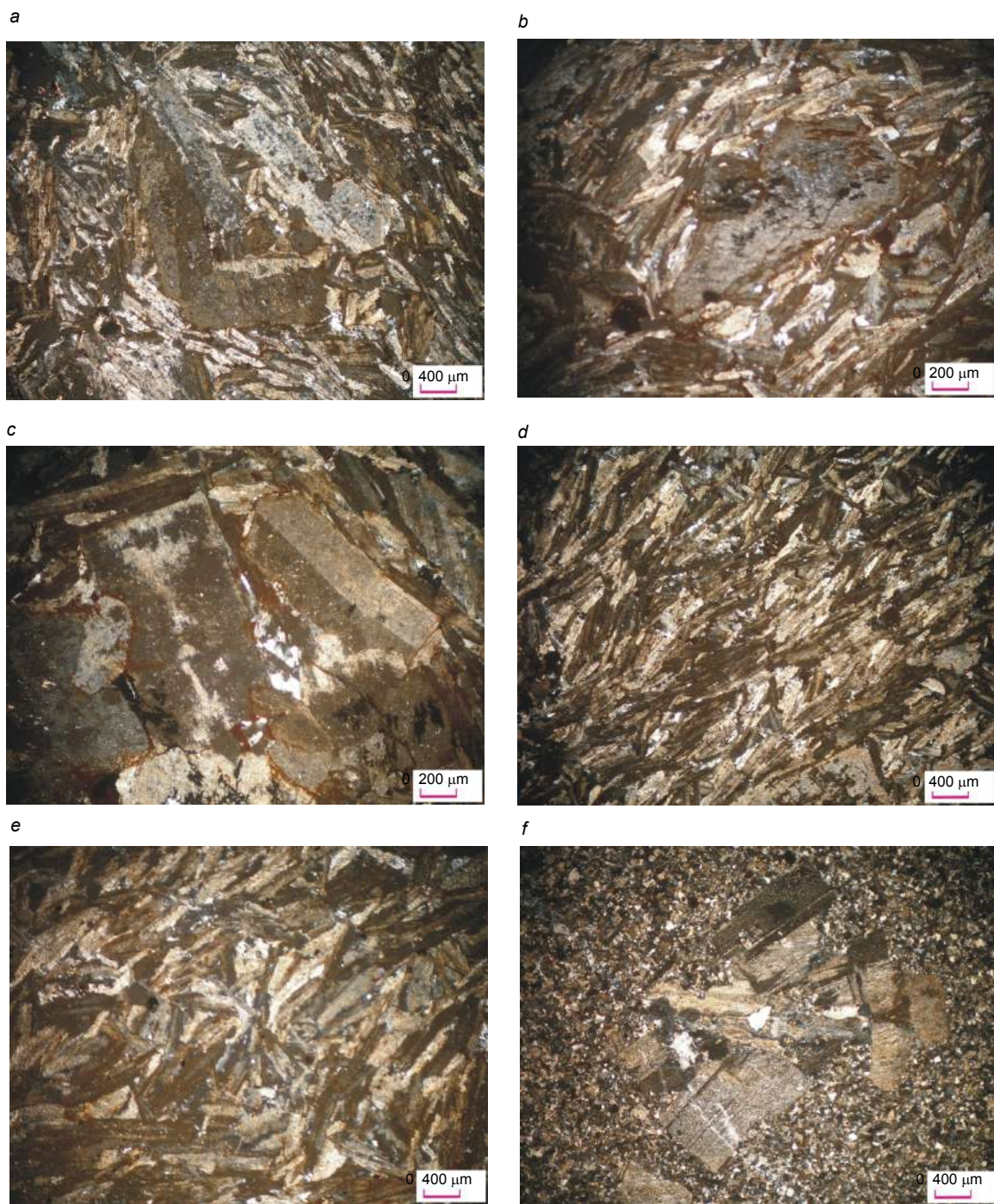


**Figure 2. Photomicrographs of trachyte dikes under crossed nicols showing.** *a* – phenocryst of K-feldspars (orthoclase and perthite) with matrix of sanidine and orthoclase; *b* – phenocryst of sanidine (with penetration twinning) embedded in a very fine grained matrix, a matrix of anorthoclase and sanidine; *c* – phenocrysts of orthoclase with simple twinning and perthite enclosing quartz; *d* – K-feldspar forming trachytic texture; *e* – randomly oriented K-feldspar crystals forming spherulitic texture; *f* – plagioclase crystals clustered to form glomeroporphyritic texture.

**Рисунок 2. Фотографии шлифов даек трахита с анализатором.** *а* – фенокрист калиевого полевого шпата (ортоклаз и перитты) в матрице санидина и ортоклаза; *б* – фенокрист санидина (со сложным двойникованием) в тонкозернистой матрице анортоклаза и санидина; *с* – фенокристы ортоклаза с простым двойникованием и пертитами, обрастающими кварц; *д* – калиевый полевой шпат, формирующий текстуру трахита; *е* – разноориентированные кристаллы калиевого полевого шпата, формирующие сферолитовую текстуру; *ф* – кристаллы плагиоклаза, сгруппированные с образованием гломеропорфировой текстуры.

(LILE) and (HFSE) elements and depletion of P, Ti and K. The depletion of Ti and p is ascribed to fractionation of titanomagnetite and apatite.

#### Magma Type

Several discrimination diagrams were proposed and used to distinguish and elucidate the magma types of the volcanic rocks.

The trachyte dykes can be subdivided generally into two major subgroups: alkali rock series and sub-alkaline (non alkali) rock series. Using [11], the dividing curve which is considered to give a better separation between alkalic and sub-alkalic rocks for general studies. It is evident that the trachyte samples fall entirely in the alkaline field (Fig. 5).

**Table 1. Chemical analyses of major oxides (wt. %), CIPW normative values (ppm) and trace element of trachyte dykes G. Umm Salatit area, CED, Egypt.**

**Таблица 1. Химический состав оксидов (вес. %), нормативные значения CIPW (г/т) и микроэлементы в дайках трахита из горного района Умм Салатит (Центральная часть Восточной пустыни, Египет).**

Oxides	Numbers						
	1	2	3	4	5	6	7
<i>Major Oxides (wt. %)</i>							
SiO <sub>2</sub>	66.39	64.09	66.24	65.54	64.58	65.14	64.54
Al <sub>2</sub> O <sub>3</sub>	13.6	15.3	13.32	15.21	15.8	12.68	12.79
TiO <sub>2</sub>	1.71	1.08	0.22	0.25	0.2	0.5	1.27
Fe <sub>2</sub> O <sub>3</sub>	5.91	6	4.78	5.52	4.35	6.36	6.66
MgO	0.4	0.3	0.23	0.61	0.12	0.55	1.33
CaO	0.9	1.1	1.68	1.13	0.64	2.2	1.13
Na <sub>2</sub> O	6.18	5.62	6.43	6.26	6.5	7.9	9.1
K <sub>2</sub> O	4.1	5.2	5.4	4.8	6.55	3.8	2.7
MnO	0.16	0.05	0.24	0.14	0.11	0.09	0.11
P <sub>2</sub> O <sub>5</sub>	0.4	0.01	0.03	0.05	0.05	0.26	0.32
LOI	0.7	1.3	1.2	0.3	1.4	1.1	0.7
Total	100.44	100.04	99.78	99.81	100.29	100.58	100.65
<i>CIPW normative values</i>							
Qtz	14.5	9.5	9.7	9	3.2	7.6	6.05
Or	24.2	30.7	31.9	28.4	38.7	23	16
Ab	48.8	47.5	38.4	51.5	44.8	43.5	50.7
An	0	1.7	0	0	0	0	0
Ac	3.012	0	13.8	1.2	8.9	18.4	19.2
Di	0	0.92	1.3	3.2	0.64	2.9	0
Il	0.3	0.1	0.4	0.2	0.2	0.1	0.2
Hm	4.8	6	0	5.07	1.2	0	0
Ap	1.04	0.02	0.07	0.1	0.1	0.6	0.7
Hy	0.9	0.7	0	0	0	0	3.3
Tn	1.3	2.5	0	0.2	0.18	1.2	2.4
A.I	1.04	0.96	1.2	1.01	1.12	1.3	1.3
K <sub>2</sub> O + Na <sub>2</sub> O	10.2	10.8	11.8	11.06	13.05	11.8	11.8
D.I.	87.5	87.7	80	88.9	86.7	74.1	72.75
S.I	2.4	1.8	1.4	3.5	0.7	2.9	6.7
<i>Trace Elements (ppm)</i>							
Ni	18.6	3.3	4.3	8.6	3.1	2.9	38.5
Co	23.2	0.8	1.4	2.8	1.1	6.3	23.9
U	9.1	12.4	11.2	16.8	9	6.5	5.4
As	11.9	3.7	3.2	6.4	4.8	4.7	12.1
Th	7.9	15.8	48	48.4	25.9	10.7	3.4
Sr	95	61	154	108	30	116	493
Cd	0.15	0.03	0.5	1.14	0.27	0.15	0.09
Sb	0.74	0.36	0.63	0.71	0.3	0.23	0.2
Bi	0.11	0.15	0.36	0.44	0.08	0.22	0.14
Cr	18	14	16	21	10	13	70
Ba	427	281	505	298	156	686	1827
W	1.9	0.5	2.7	5.3	1.2	1.1	0.3
Zr	145.1	85.1	1835	1952	395.7	491.9	96.6

Oxides	Numbers						
	1	2	3	4	5	6	7
Sn	1.2	2.2	20.9	18.5	6.9	5	1.6
Sc	3.5	2.2	0.9	2	0.6	5.2	9.9
Y	24.8	25.4	118.1	119.7	39.6	36.9	12.9
Hf	3.74	3.87	38.45	41.5	8.97	11.54	2.88
Li	32	8	40.5	48.4	13.2	80.2	82.3
Rb	77	134.9	208.1	12.4	12.4	79.2	27.4
Ta	0.7	2.1	24.4	22.7	11.5	2.9	0.8
Nb	22.74	23.63	388.9	308.1	170.8	44.51	10.81
Ga	25.9	21.12	52.39	56.32	37.58	26.41	18.15
Mo	2.67	1.46	2.35	9.79	5	5.84	1.21
Cu	24.56	6.1	4.95	7.85	5.41	6.13	19.39
Pb	9.65	13.85	16.98	18.45	13.88	9.43	10.74
Zn	114.5	37.2	169.5	268.8	133.1	74.5	76.7
Re	0.002	0.002	0.002	0.002	0.002	0.002	0.002
Se	0.3	0.5	0.3	0.3	0.3	0.4	0.3

**Table 2. Comparison of average chemical composition of the studied trachyte dykes with some Egyptian and world average.**

Таблица 2. Сравнение среднего химического состава изучаемых трахитовых даек с другими египетскими и мировыми комплексами.

Oxides	Numbers				
	1	2	3	4	5
SiO <sub>2</sub>	65.22	61.2	64.24	63.7	64.5
TiO <sub>2</sub>	0.76	0.7	0.25	0.17	0.4
Al <sub>2</sub> O <sub>3</sub>	14.18	16.9	13.68	15.77	13.4
Fe <sub>2</sub> O <sub>3</sub>	5.65	1.48	—	4.06	6
MgO	0.51	0.39	1.57	0.4	1
CaO	1.26	1.14	1.46	2.51	1.8
Na <sub>2</sub> O	6.86	3.55	5.8	6.38	6.6
K <sub>2</sub> O	4.67	4.3	4.09	4.62	4.6
MnO	0.13	0.06	0.1	0.18	0.2
P <sub>2</sub> O <sub>5</sub>	0.17	—	0.14	0.16	0.33

1 – trachyte dykes of G. Umm Salatit area, CED, Egypt (present work).

2 – average of world trachyte dykes [6].

3 – average of Um Domit trachytes [8].

4 – average of trachyte of G. El Ghorfa area, SED, Egypt [9].

5 – average of trachytes of Umm Shaghir, CED, Egypt [7].

AFM diagram originally constructed by [12] is commonly used for identifying iron depletion and iron enrichment trends characteristic of calc-alkalic and tholeiitic series, respectively [13]. The analyzed samples were plotted on the AFM diagram using the dividing line suggested by [11] to separate tholeiitic and calc-alkaline composition. All the studied samples fall within the calc-alkalic field with 1971. Compressional and tensional trends (after [14]) (Fig. 6, a).

### Tectonic Setting

An attempt is made here to identify the tectonic environment of the studied trachyte based on the presently popular discrimination diagrams using major and trace elements data [15] constructed (Al<sub>2</sub>O<sub>3</sub>/TiO<sub>2</sub>) versus TiO<sub>2</sub> variation diagram (Fig. 6, b). The analysed trachyte samples show complete spectra of values of the completely volcanic suite that fall along the same trend. This may suggest that samples were derived from the same magma source by fractionation processes with high TiO<sub>2</sub> magma being the early fractionated while the lower TiO<sub>2</sub> magma is produced from more fractionated varieties. The relation between the SiO<sub>2</sub> and Ba/Nb ratio (Fig. 6, c) shows a decrease of the Ba/Nb ratio as a function of differentiation in the studied trachyte. This indicating that the high Ba/Nb in the most primitive rocks is a characteristic feature inherited from their source.

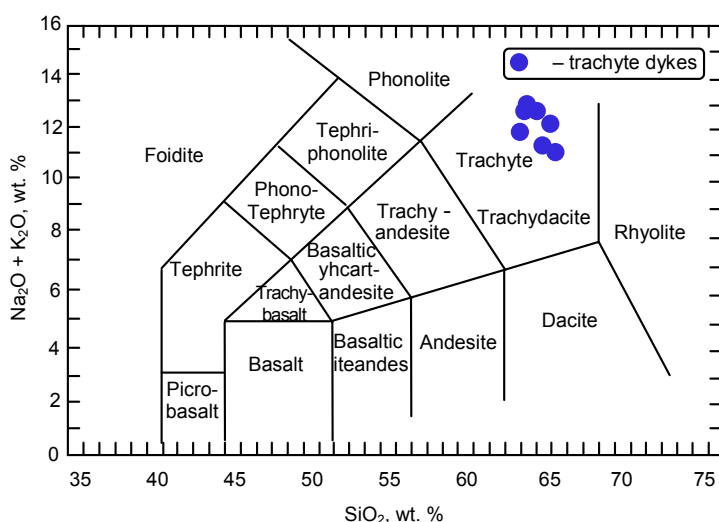


Figure 3.  $\text{Na}_2\text{O} + \text{K}_2\text{O}$  versus  $\text{SiO}_2$  (after [5]).  
Рисунок 3. Диаграмма  $\text{Na}_2\text{O} + \text{K}_2\text{O} - \text{SiO}_2$  (по [5]).

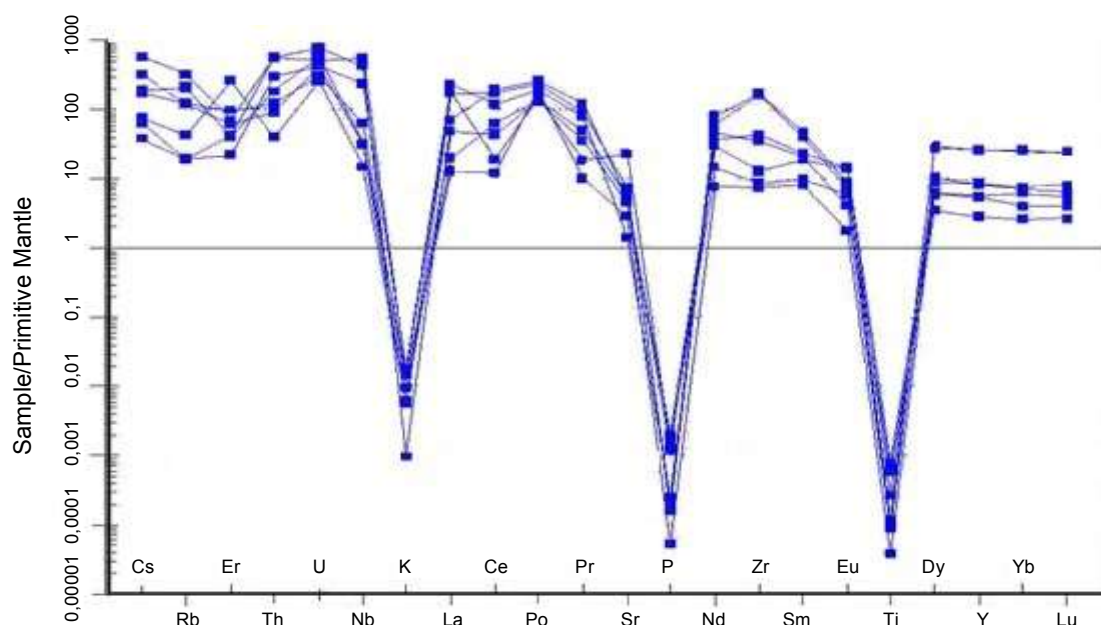


Figure 4. Normalized multi-elements patterns of the trachyte dykes, G. Umm Salatit area, CED, Egypt. Normalized to the primitive mantle values [10].

Рисунок 4. Нормализованные мульти-элементные кривые для трахитовых даек, Умм Салатит, Центральная часть Восточной пустыни, Египет. Нормализовано к значениям примитивной мантии [10].

#### Rare Earth Elements (REEs) geochemistry

The distribution of europium (Eu) is particularly important because it can occur in two oxidation states, divalent ( $\text{Eu}^{+2\text{P}}$ ) and trivalent ( $\text{Eu}^{+3\text{P}}$ ) depending on oxygen fugacity. Under oxidizing conditions, Eu is trivalent and behaves as the other rare earth elements, while under reducing conditions, it occurs as divalent  $\text{Eu}^{+2\text{P}}$ , which has relatively large ionic radius and replace mainly  $\text{Ca}^{+2\text{P}}$  in plagioclases and rarely  $\text{KP}^{+3\text{P}}$  in K-feldspar. The average normalized REE patterns of Umm Salatit trachyte dykes display low to moderate fractionated REE pattern (Table 3), (Fig. 7) relative to chondritic values from [16] where the averages  $(\text{La/Yb})_n = 16.8$  and have marked enrichment of the average of  $\Sigma\text{LREE}$  (324.6) relative to the average of  $\Sigma\text{HREEs}$  (26.4) where the averages  $(\text{La/Sm})_n = 5.6$ . trachyte dykes have moderate negative Eu anomaly ( $\text{Eu}/\text{Eu}^* = 0.5$ ), this may reflect the plagioclase and K-feldspar fractionation or due to the greater effect and higher oxygen activity of the melt, which is relates to volatile saturation (higher oxidation state) in case of the melt that formed the melt. The oxygen activity of the melt would be sufficiently high to keep Eu at the trivalent state and thus keep its incorporation into accumulating plagioclase [17].

The dose rate in the trachyte dykes ranges from 0.5 to 1.5 with an average of 1.2 (m Sv/y). The radiometric data of the radio-elements for them show a wide variation in eU and eTh contents. The eU content ranges from 2 to 14 ppm with an average of 6.6 ppm and the eTh content ranges from 4 to 37 ppm with an average of 18.03 ppm. The potassium content is ranging between 1.9 % and 5.1% with an average of 3.4%.

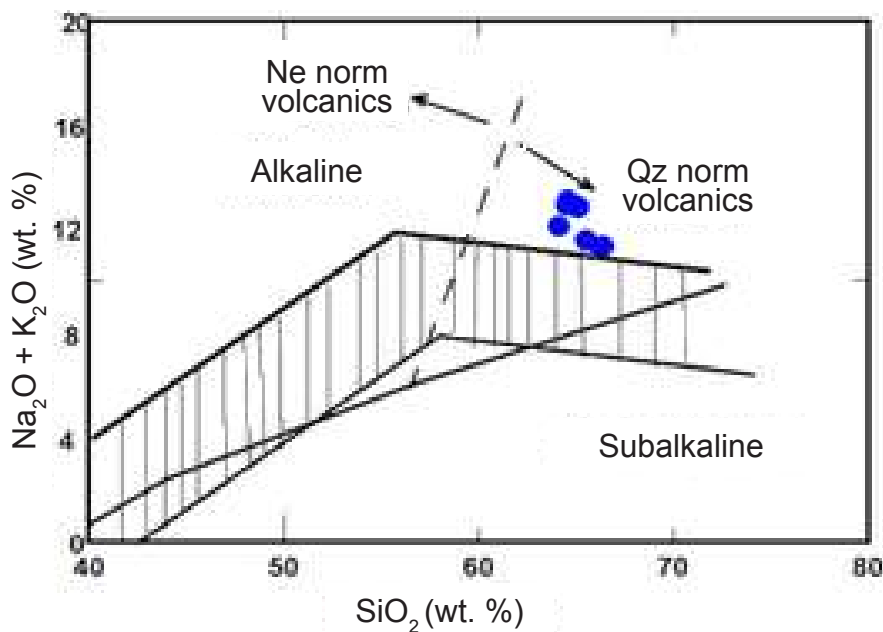
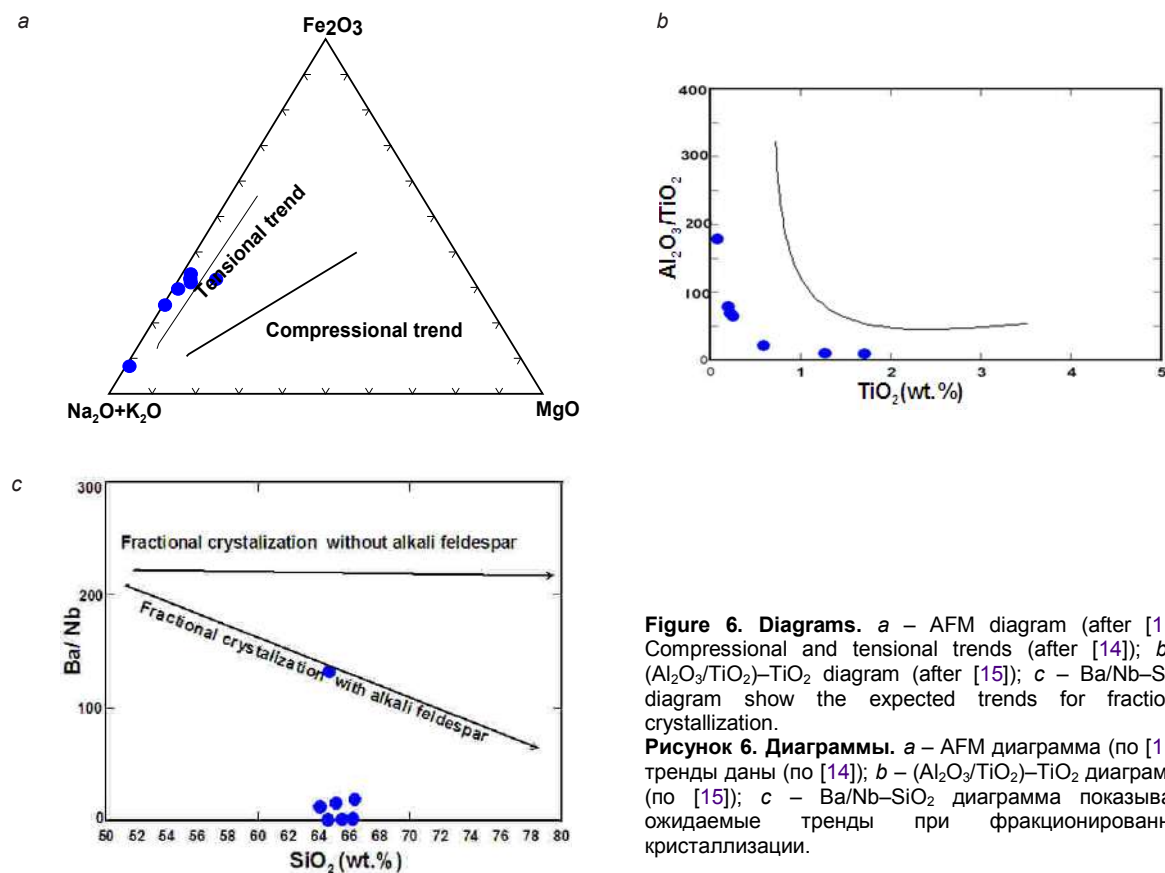


Figure 5. Alkali-silica variation diagram, the dividing curve after [11].  
Рисунок 5. Диаграмма  $\text{Na}_2\text{O} + \text{K}_2\text{O}$  -  $\text{SiO}_2$ , разделительная кривая по [11].

Table 3. The REEs contents (ppm) of the studied trachyte dykes G. Umm Salatit area, CED, Egypt.

Таблица 3. Содержание редкоземельных элементов (г/т) в трахитовых дайках Умм Салатит (Центральная часть Восточной пустыни, Египет).

REEs	Numbers							Aver.
	1	2	3	4	5	6	7	
La	33.4	8.9	119.5	49.7	161.5	14	122.2	72.7
Ce	78.73	21.92	313.4	348.5	211	112.3	34.19	160.0
Pr	9.9	2.8	25.7	33.6	22	13.9	5.1	16.1
Nd	40.1	10.5	84.7	113.2	63	50.9	20	54.6
Sm	8.5	3.6	18	21	9.3	10.6	4.4	10.8
Eu	2.4	0.3	1.3	1.5	0.7	2.5	1	1.4
Gd	7.7	3.6	15.9	16.7	5.2	9.5	4	8.9
Tb	0.9	0.7	3.6	3.6	1.1	1.5	0.5	1.7
Dy	4.3	4.7	22.1	20.7	6.6	7.8	2.6	9.8
Ho	0.9	0.9	4.3	4.5	1.5	1.5	0.5	2.0
Er	2.1	2.6	12.3	13.3	4.2	3.7	1.2	5.6
Tm	0.3	0.5	1.9	2	0.7	0.5	0.2	0.9
Yb	2	3.1	12.4	13	3.7	3.4	1.3	5.6
Lu	0.3	0.4	1.8	1.8	0.6	0.5	0.2	0.8
$\Sigma$ REE	191.5	64.5	636.9	643.1	491.1	232.6	197.4	351.0
$\Sigma$ LREE	180.7	51.6	578.5	584.2	472.7	213.7	190.9	324.6
$\Sigma$ HREE	10.8	12.9	58.4	58.9	18.4	18.9	6.5	26.4
$\Sigma$ LREE/ $\Sigma$ HREE	16.7	4.0	9.9	9.9	25.7	11.3	29.4	15.3
Eu/Eu*	0.9	0.3	0.2	0.2	0.3	0.8	0.7	0.5
(La/Yb)n	11.26	1.94	6.5	2.58	29.43	2.78	63.37	16.8
(La/Sm)n	2.5	1.6	4.2	1.5	10.9	0.8	17.5	5.6
(Ce/Sm)n	2.24	1.47	4.2	4.01	5.48	2.56	1.88	3.1
(Eu/Yb)n	3.4	0.3	0.3	0.3	0.5	2.1	2.2	1.3
(Ce/Sm)n	2.2	1.5	4.2	4.0	5.5	2.6	1.9	3.1



**Figure 6. Diagrams.** a – AFM diagram (after [11]). Compressional and tensional trends (after [14]); b – (Al<sub>2</sub>O<sub>3</sub>/TiO<sub>2</sub>)–TiO<sub>2</sub> diagram (after [15]); c – Ba/Nb–SiO<sub>2</sub> diagram show the expected trends for fractional crystallization.

**Рисунок 6. Диаграммы.** а – AFM диаграмма (по [11]), тренды даны (по [14]); б – (Al<sub>2</sub>O<sub>3</sub>/TiO<sub>2</sub>)–TiO<sub>2</sub> диаграмма (по [15]); в – Ba/Nb–SiO<sub>2</sub> диаграмма показывает ожидаемые тренды при фракционированной кристаллизации.

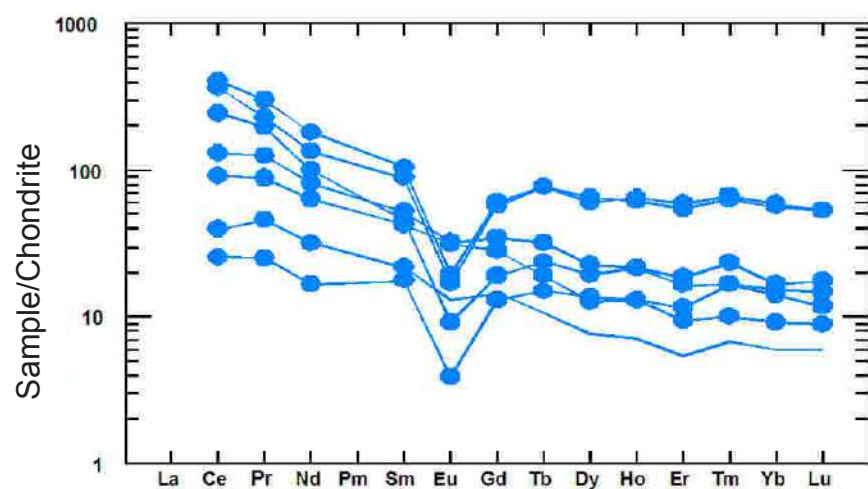


**Figure 7. Normalized REE patterns of the trachyte dyke, G. Umm Salatit area, CED, Egypt. The chondritic values are from [16].**

**Рисунок 7. Нормализованные на хондрит РЗЭ кривые для трахитовых даек, Умм Салатит, Центральная часть Восточной пустыни, Египет. Хондритовые значения взяты из [16].**

#### Distribution of Radioelements in Trachyte Dykes

The relationship between eU with eTh, eTh with K%, the eU with eU/eTh contents among the trachyte dykes reflect a direct relation that means the eU/eTh ratio tends to increase with uranium mobilization and post magmatic redistribution in trachyte dykes (Fig. 8).

#### The correlation matrix between U, Th (chemically) and some major, traces and rare earth elements

For trachyte dykes both U and Th correlate similarly with other major, trace and rare earth elements, reflecting their geochemical coherence during the crystallization of the magma (Fig. 10–12).

#### Conclusion

1. Macroscopically, Trachyte dykes are fine to medium grained of buff and pale pink to red in colour. Microscopically, consist mainly of K-feldspar with relatively few plagioclase, iron oxides, quartz and biotite. Secondary minerals are represented by sericite, muscovite, chlorite, carbonates and epidote. Accessory minerals are represented by zircon and opaque minerals.

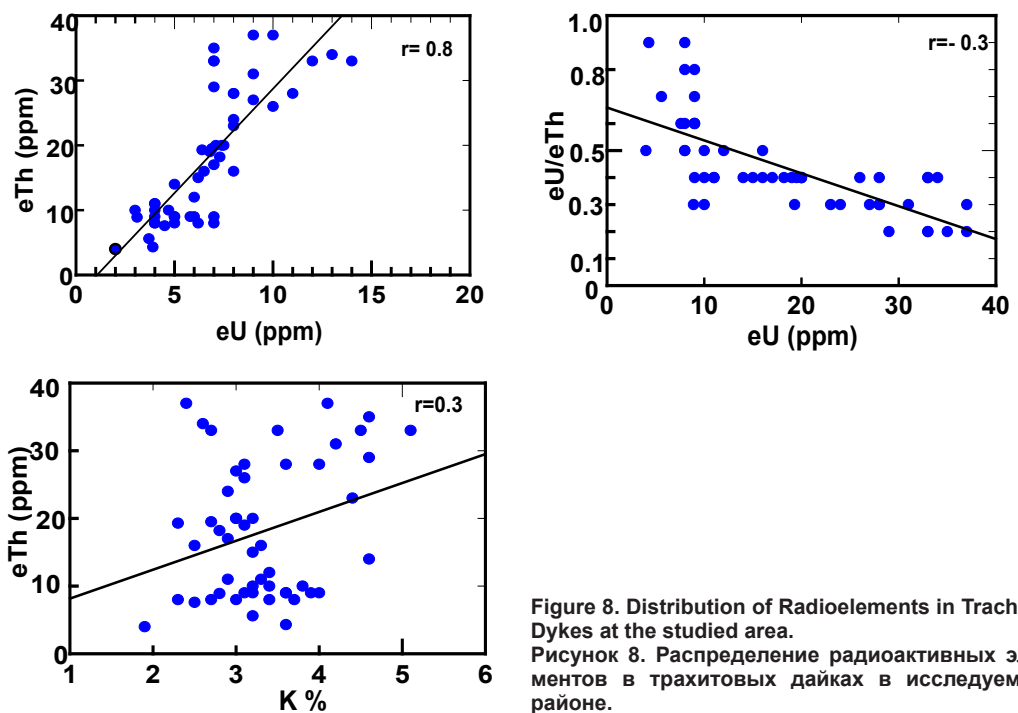


Figure 8. Distribution of Radioelements in Trachyte Dykes at the studied area.

Рисунок 8. Распределение радиоактивных элементов в трахитовых дайках в исследуемом районе.

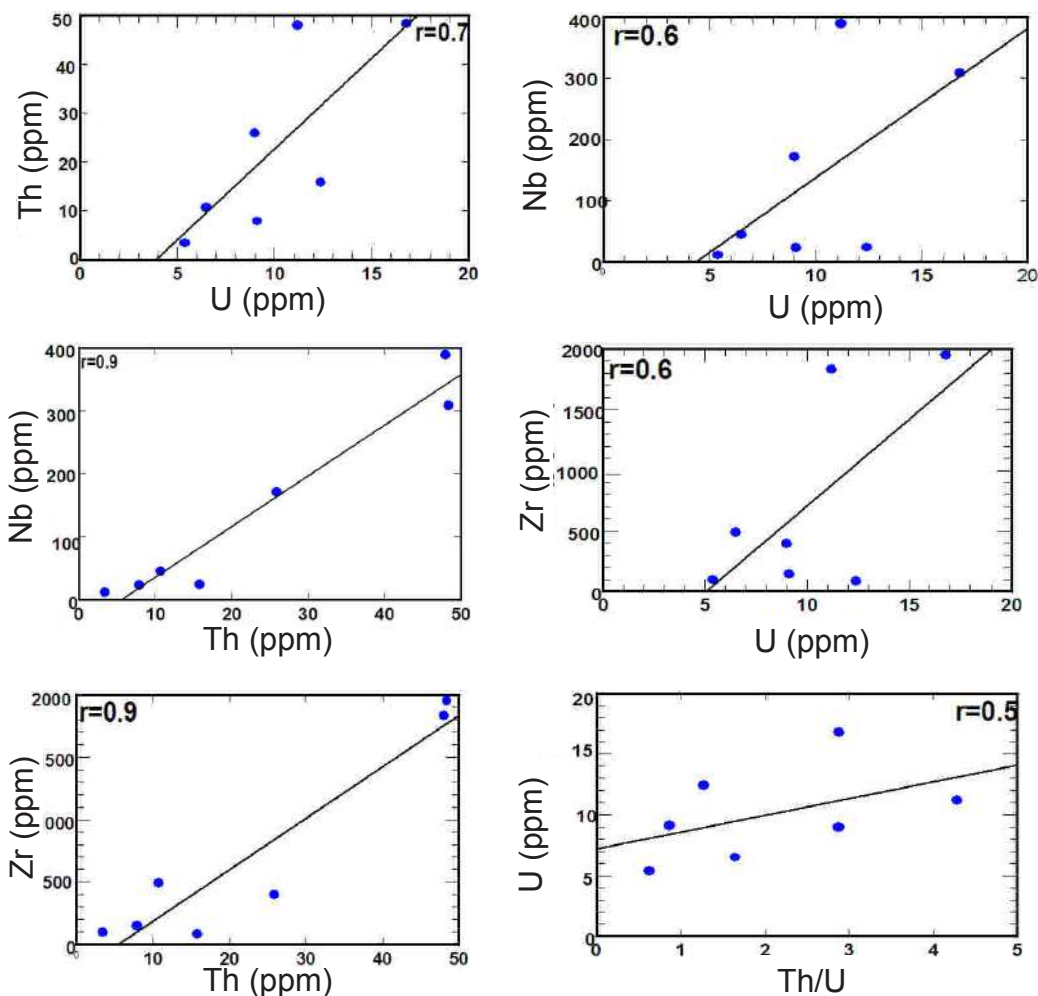


Figure 9. Binary relations between U-Th, U-Zr, U-Nb, Th-Zr and Th-Nb for the studied trachyte dykes at G. Umm Salatit area, CED, Egypt.

Рисунок 9. Бинарные отношения между U-Th, U-Zr, U-Nb, Th-Zr и Th-Nb для изучаемых трахитовых даек в районе Умм Салатит, Центральная часть Восточной пустыни, Египет.

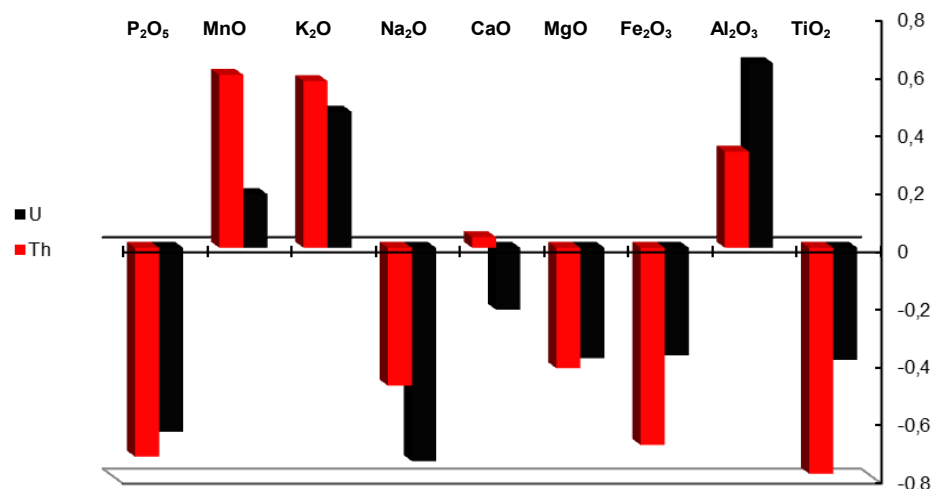


Figure 10. Bar diagram showing the correlation coefficients of some major elements with U and Th measured chemically for trachyte dykes of G. Umm Salatit, CED, Egypt.

Рисунок 10. Столбчатая диаграмма, показывающая коэффициенты корреляции некоторых основных элементов с U и Th, измеренных химически для трахитовых даек Умм Салатит, Центральная часть Восточной пустыни, Египет.

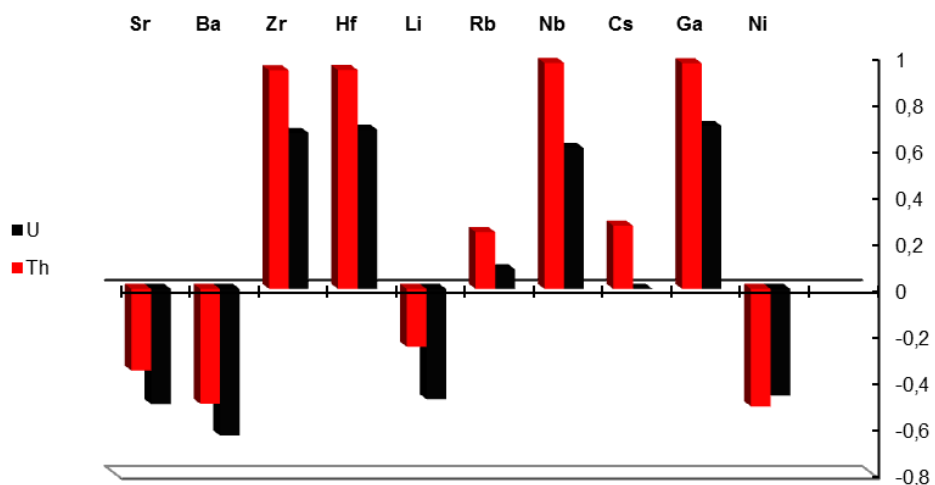


Figure 11. Bar diagram showing the correlation coefficients of some trace elements with U and Th measured chemically for trachyte dykes of G. Umm Salatit, CED, Egypt.

Рисунок 11. Столбчатая диаграмма, показывающая коэффициенты корреляции некоторых микроэлементов с U и Th, измеренными химически для трахитовых даек Умм Салатит, Центральная часть Восточной пустыни, Египет.

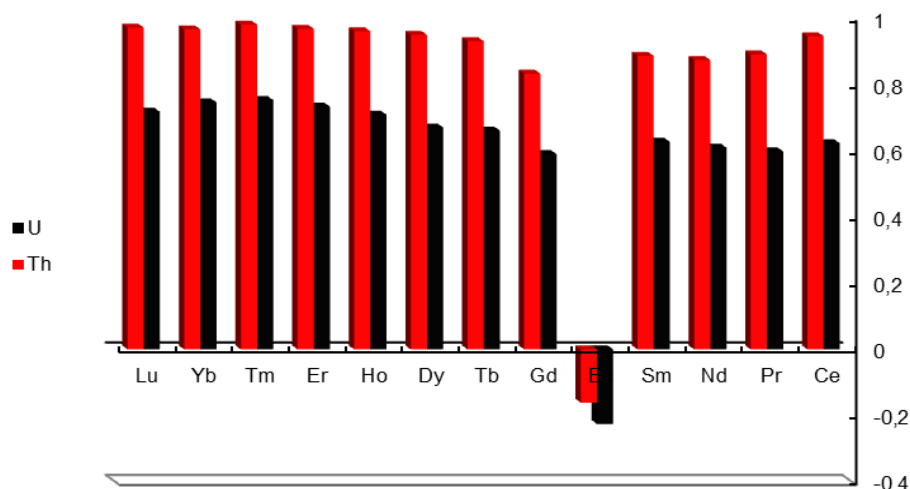


Figure 12. Bar diagram showing the correlation coefficients of some rare earth elements (REEs) with U and Th measured chemically for trachyte dykes of G. Umm Salatit, CED, Egypt.

Рисунок 12. Столбчатая диаграмма, показывающая коэффициенты корреляции некоторых редкоземельных элементов (РЗЭ) с U и Th, измеренных химически для трахитовых даек Умм Салатит, Центральная часть Восточной пустыни, Египет.

2. Geochemically, the investigated trachyte dykes were originated from an alkali magma rich in total alkalis, and the tectonic setting is continental basalt. Trachyte dykes have steep LREEs, nearly flat HREEs and a negative Eu anomaly. The negative Eu anomaly is either due to the partitioning of Eu into feldspar during fractionation, which is an important process in developing alkalinity, or the presence of residual feldspar in the source. Another alternative explanation for the negative Eu anomaly is based on the high oxygen fugacity in the melt due to volatile saturation.

3. The dose rate in the trachyte dykes ranges from 0.5 to 1.5 with an average of 1.2 (m Sv/y). The radiometric data of the radioelements for them show a wide variation in eU and eTh contents. The eU content ranges from 2 to 14 ppm with an average of 6.6 ppm and the eTh content ranges from 4 to 37 ppm with an average of 18.03 ppm.

4. Both U and Th correlate similarly with other major and trace elements, their geochemical coherence during the crystallization of the magma.

#### REFERENCES

1. Ghoneim M. M. 2014, Geology and uranium potentiality of Gabal Umm Salatit Environ, Central Eastern Desert, Egypt. M. Sc. Thesis, Faculty of Science, Minya University, p. 168.
2. Mansour M. S., Bassuni F. A. and El-Far D. M. 1956, Geology of Umm Salatit El-Hisnat district, Geol. Surv. Egypt, p. 43.
3. Barker D. S. 1970, Compositions of granophyre, myrmekite, and graphic granite. Bulletin of the Geological Society of America, 81:3339–3350.
4. Lentz D. R., Fowler A. D. 1992, A dynamic model for quartz-feldspar graphic intergrowths from granitic pegmatites in the southwestern Grenville Province. *The Canadian Mineralogist*, 30 (3): 571–585.
5. Cox K. G., Bell J. D. and Pankhurst R. J. 1979, The interpretation of igneous rocks. London, Allen and Unwin, p. 450.
6. Le Maitre R. W. 1989, A classification of igneous rocks and glossary terms: Recommendations of the international Union of Geological Sciences sub commission on the systematic of igneous rocks. Blackwell Scientific Publ., Oxford, p. 193.
7. Gharib M. E., Obeid M. A. and Ahmed A. H. 2012, Paleozoic alkaline volcanism: geochemistry and petrogenesis of Um Khors and Um Shaghir trachytes of the central Eastern Desert, Egypt, Arab J. Geosci, 5:53–71.
8. Saleh G. M., Ibrahim I. H., Azab M., Abdel Wahed A. A., Ragab A. A. and Ibrahim M. E. 2004, Geologic and spectrometric studies on Um Domi Phanerozoic trachyte plug, South Eastern Desert, Egypt. The 6<sup>th</sup> Intern. Conf. on Geochemistry, Alex. Univ., Egypt, pp. 329–345.
9. EL Tohamy A. M. 2011, Mineralogy and geochemistry of the volcanic rocks of Gabal El Ghorfa, South Eastern Desert, Egypt, M. Sc. Thesis, Faculty of Science, Benha University, p. 202.
10. Sun S. S. and McDonough W. F. 1989, Chemical and isotopic systematic of oceanic basalts: implications for mantle composition and processes. In Saunders A. D., Norry M. J. (eds.), Magmatism in the ocean Basins. Geological Society Special Publication. 42:313–345.
11. Irvine T. J. and Baragar W. R. 1971, A guide to the chemical classification of the common volcanic rocks. Canadian Journal of Earth Science 8:523–548.
12. Wager L. R. and Deer W. A. 1939, The petrology of the Skaergaard intrusion, East Greenland. Meddel. om Gronland, 10: 52.
13. Kuno H. 1966, Lateral variation of basalt magma type across continental margin and island arcs. Bull. Volcanol., 29:195–222.
14. Petro W. L., Vogel T. A. and Wilband J. T. 1979, Major element chemistry of plutonic rock suites from compressional and extensional plate boundaries. Chem. Geol., Vol. 26, pp. 217–235.
15. Sun S. S. and Nesbit R. W. 1978, Petrogenesis of Archean ultrabasic and basic volcanics: evidence from rare earth elements. Contrib. Mineral. Petrol., 65:301–325.
16. Boynton W. V. 1984, Geochemistry of the rare earth elements: meteorite studies In: Henderson, P. (ed.) Rare earth element geochemistry [M]. Elsevier, Amsterdam, pp. 63–114.
17. Grenne T. and Roberts D. 1998, The Holonda porphyrite, Norwegian Caledonides: geochemistry and tectonic setting of Early-Mid. Ordovician shoshonite volcanism. J. Geol. Soc., London, 155:131–142.

*The article was received on February 14, 2018*

# Геохимия, уран, торий и редкоземельные элементы трахитовых даек горного района Умм Салатит Центрально-Восточной пустыни, Египет

**Мохамед Махмуд Гхонеим<sup>1,2</sup>,**

moh.gho@mail.ru

**Гехад Мохамед Салех<sup>2</sup>,**

drgehad\_m@yahoo.com

**Махер Давуд Давуд<sup>3</sup>,**

dawoud\_99@yahoo.com

**Мохамед Салех Азаб<sup>2</sup>,**

mohamedazab68@yahoo.com

**Махмуд Ахмед Мохамед<sup>2</sup>,**

hoodageo@yahoo.com

**Хамди Ахмед Авад<sup>4,5</sup>**

hamdiawaad@gmail.com

<sup>1</sup>Санкт-Петербургский государственный университет

Санкт-Петербург, Россия

<sup>2</sup>Управление ядерных материалов

Каир, Египет

<sup>3</sup>Университет Минуфия

Минуфия, Египет

<sup>4</sup>Южный Федеральный университет

Ростов-на-Дону, Россия

<sup>5</sup>Университет аль-Азхар

Асъют, Египет

Горный район Умм Салатит – часть Центрально-Восточной пустыни в Египте. Он состоит из офиолитового меланжа, древних гранитоидов, биотитовых гранитов, мусковитовых гранитов и постгранитных даек и жил.

**Цель работы.** Настоящая работа посвящена детальным исследованиям геологии, петрографии, геохимии и спектрометрическим изысканиям изучаемых трахитовых даек в качестве возможного источника минерализации урана.

**Методы исследования.** Исследование подразумевает как работу в поле (построение геологической карты со структурными особенностями, масштаб 1 : 50 000, спектрометрические измерения различного комплекса горных пород с помощью портативного гамма-спектрометра RS-230), так и лабораторные работы (подготовка разрезов для петрографических исследований и их изучение с помощью поляризационного микроскопа), атомно-эмиссионной спектроскопии (AES), а также масс-спектрометрии с индуктивно связанным плазмой (ICP-MS).

**Результаты.** Петрографически дайки трахитов состоят из К-полевого шпата с относительно небольшим количеством плахиоклаза, оксидов железа, кварца и биотита. Вторичные минералы представлены серицитом, мусковитом, хлоритом, карбонатами и эпидотом. Аксессорные минералы – это непрозрачные минералы. Трахитовые текстуры являются основной характерной особенностью трахита. Геохимически исследованные трахитовые дайки образовались из щелочной магмы, богатой щелочными металлами, а тектонически расположены среди континентальных базальтов. Трахитовые дайки характеризуются кругонаклонным распределением легких редкоземельных элементов и почти горизонтальным распределением тяжелых редкоземельных элементов и имеют отрицательную аномалию в области Eu. Отрицательная Eu аномалия связана либо с разделением Eu в полевых шпатах в процессе фракционирования расплава, что является важным процессом развития щелочности, либо с наличием остаточного полевого шпата в магматическом очаге. Другое альтернативное объяснение отрицательной Eu аномалии связано с высокой фугитивностью кислорода в расплаве из-за насыщения газом. В целом все образцы трахитов демонстрируют умеренное обогащение большинством крупно-ионных литофильных элементов (LILE) и высокозарядных элементов (HFSE) и истощение по Р, Ti и K. Истощение Ti и P связано с фракционированием титаномагнетита и апатита в расплаве. Определение эквивалентного урана, тория (в г/т), калия (в %) и мощности радиометрической дозы (мЗв/год) с использованием портативного RS-230 указывает на то, что мощность дозы в дайках трахита колеблется от 0,5 до 1,5 со средним значением 1,2 (мЗв/год). Радиометрические данные радиоактивных элементов показывают широкую вариацию содержания eU и eTh. Содержание eU составляет от 2 до 14 г/т, в среднем 6,6 г/т, а содержание eTh составляет от 4 до 37 г/т со средним значением 18,03 г/т и Th коррелируют аналогично другим основным и микроэлементам, отражающим их геохимическую связь во время кристаллизации магмы.

**Ключевые слова:** геохимия, уран, трахитовые дайки, Египет, Умм Салатит.

Статья поступила в редакцию 14 февраля 2018 г.